Thermochimica Acta 485 (2009) 65–71

Contents lists available at ScienceDirect

Thermochimica Acta

journal homepage: www.elsevier.com/locate/tca

Thermal degradation mechanism of HDPE nanocomposites containing fumed silica nanoparticles

K. Chrissafis [a], K.M. Paraskevopoulos [a], E. Pavlidou [a], D. Bikiaris [b,*]

[a] Solid State Physics Section, Physics Department, Aristotle University of Thessaloniki, GR-541 24 Thessaloniki, Macedonia, Greece
[b] Laboratory of Organic Chemical Technology, Department of Chemistry, Aristotle University of Thessaloniki, GR-541 24 Thessaloniki, Macedonia, Greece

ARTICLE INFO

Article history:
Received 23 October 2008
Received in revised form 8 December 2008
Accepted 9 December 2008
Available online 24 December 2008

Keywords:
Polyethylene
Nanocomposites
Fumed silica
Thermal stability
Degradation mechanism

ABSTRACT

In the present study different series of high-density polyethylene (HDPE) nanocomposites, containing 0.5, 1, 2.5 and 5 wt.% of fumed silica (SiO_2) nanoparticles were prepared by melt-mixing on a Haake–Buchler Reomixer. From SEM micrographs it was found that even though there is a fine dispersion of nanoparticles into HDPE matrix there are also some aggregates formed and their size depends directly on the SiO_2 content. Tensile strength increases by increasing silica content up to 2.5 wt.% SiO_2, while at 5 wt.% a reduction was observed. Additionally, Young's modulus increases continuously while impact strength has the opposite trend and SiO_2 content has no monotonic effect on HDPE melting point. Thermal stability of HDPE was enhanced due to the incorporation of SiO_2 nanoparticles. From the kinetic analysis of thermal decomposition of HDPE and its nanocomposites, it was concluded that in order to describe the thermal degradation mechanism, two consecutive mechanisms of *n*th-order (Fn) and *n*th-order with autocatalysis (Cn) have to be considered. SiO_2 have no effect on decomposition mechanism but only to the activation energies, which in nanocomposites are higher, compared with neat HDPE, due to the stabilization effect of SiO_2 nanoparticles.

1. Introduction

High-density polyethylene (HDPE) is a semicrystalline polymer ideal for many industrial applications such as packaging materials, pipes, bottles, etc. [1]. HDPE pipes have many advantages compared with others such as light weight, low thermal conductivity, high toughness and impact strength, resistance to abrasion, corrosion resistance and are inert to the most of chemicals. Due to their non-toxicity, and longer life cycle they are used mainly for water supply and gas transmission, in agriculture and in chemical industries. Grade material PE-80 and PE-100 are the most versatile material suitable for pipes. These materials should have low gas permeability and thermal stability. From our previous study it was found that the addition of nanoparticles including montmorillonite (MMT), SiO_2 and multi-walled carbon nanotubes can increase both of these properties [2]. Furthermore, it was reported that the addition of such nanoparticles could increase, also, the mechanical properties of HDPE such as tensile modulus and impact strength [3–15]. However, limited are the studies concerning their effect on thermal degradation. From our previous works it was found that the addition of SiO_2 nanoparticles could increase the thermal stability of many polymers [16,17]. So, in the present study HDPE/SiO_2 nanocomposites containing different SiO_2 content were prepared in order to evaluate the effect of these nanoparticles on thermal decomposition of HDPE as well as on its mechanical properties.

Polyethylene decomposes into a large number of paraffinic and olefinic compounds without a residue. Wu et al. [18] calculated with non-isothermal TGA measurements that the activation energy is 233.2 kJ mol^{-1} and the reaction order $n = 0.74$ using reaction order kinetic model for the fitting of the experimental data. Knumann and Bockhorn [19] and Bockhorn et al. [20,21] by means of TG:MS have determined an apparent energy of activation E_α of 262.1 kJ mol^{-1}, a decimal logarithm of the pre-exponential factor $\log(k_0/\text{min}^{-1})$ of 18 and an apparent order of reaction of 0.83. Park et al. [22] using a new dynamic method for non-isothermal measurements with different heating rates have calculated the apparent activation energy (333.2–343.2 kJ mol^{-1}) and the reaction order *n* (0.93–0.98).

Concerning the thermal degradation mechanism of polyethylene, Ballice [23] differentiated the formation of 1-olefins and n-paraffins and calculated the activation energy of them, 124.7 ± 4 and 41.6 ± 2 kJ mol^{-1}, respectively, using non-isothermal measurements. Also, using Flynn and Wall method he calculated the apparent activation energy (average $E = 238.4 \pm 2$ kJ mol^{-1}) while by Yang et al. [24] similar activation energies (240–264 kJ mol^{-1}) were mentioned. Araujo et al. [25] using the Vyazovkin model, determined the activation energy as 290 kJ mol^{-1} while lower activation

* Corresponding author. Tel.: +30 2310 997812; fax: +30 2310 997667.
E-mail address: dbic@chem.auth.gr (D. Bikiaris).

0040-6031/$ – see front matter © 2008 Elsevier B.V. All rights reserved.
doi:10.1016/j.tca.2008.12.011

energies were reported by Gao et al. [26] using non-isothermal and isothermal measurements (194.8 and 201.5 kJ mol^{-1}, respectively).

Kim et al. [27] introduced the peak property method for the estimation of the activation energy, the pre-exponential factor and the reaction order (power law models) from a single derivative thermogravimetry curve. The calculated values of the activation energy, for different heating rates, were in the range 231.4 ± 11.9 to 278.6 ± 13.4 kJ mol^{-1} and the reaction order from 0.554 to 0.604. Sinfronio et al. [28] used different methods for the estimation of the activation energy (Ozawa–Flynn–Wall, Van Krevelen, Horowitz–Metzger, Coats–Redfern, Madhusudanan) and power law models for single heating rate data. The area of the calculated values was from 200 to 270 kJ mol^{-1} and for the reaction order from 0.41 to 0.65. They used also the isoconversional methods OFW and Vyazovkin and the area of the values of the activation energy for the conversions of 0.1 till 0.9 was 162.5–230.5 and 279.6–293.4 kJ mol^{-1}, respectively.

From the above literature study it appears that although a lot of work has been published for the kinetic study of HDPE thermal degradation, the values of activation energy appear to have a lot of variations. This is, mainly, attributed to the different methods that were used for their calculations. Simultaneously, these activation energies were calculated using the data from only a single heating rate and were used different methods with predetermined kinetic model (F1 or Fn). These models have been used widely to study the thermal degradation of polymers because they are very simple, although the reaction mechanism of polymer decomposition is a very complex radical chain mechanism, including initiation, propagation and termination reactions. Furthermore, even though there are a lot of papers dealing with polyethylene nanocomposites, the effect of nanoparticles on thermal decomposition mechanism is not studied yet.

The aim of the present study was to evaluate the effect of fumed silica nanoparticles on the properties and mainly on thermal degradation mechanism and decomposition rate of HDPE. Additionally, the scope of the present study is to calculate the activation energies of decomposition of neat HDPE, in comparison with that of the prepared HDPE/SiO_2 nanocomposites.

2. Experimental

2.1. Materials

Bimodal HDPE appropriate for pipe and fittings production was supplied by TVK Inter-Chemol GmbH (Frankfurt am Main, Germany) under the trade name TIPELIN 7700M and had a melt flow index (MFI) of 0.28 g/10 min at 5.0 kg/190 °C, density 0.950 g/cm^3 and T_m 127 °C. Fumed silica (SiO_2) nanoparticles having a specific surface area 200 m^2/g, average primary particle size 12 nm and SiO_2 content >99.8% used for nanocomposites preparation were supplied by Degussa AG (Hanau, Germany) under the trade name SiO_2® 200.

2.2. Nanocomposites preparation

Nanocomposites containing 0.5, 1, 2.5 and 5 wt.% of SiO_2 nanoparticles were prepared by melt-mixing in a Haake–Buchler Reomixer (model 600) with roller blades and a mixing head with a volumetric capacity of 69 cm^3. Prior to melt-mixing the nanoparticles were dried by heating in a vacuum oven at 130 °C for 24 h. The two components were physically premixed before being fed in the reomixer, in order to achieve a better dispersion of the nanoparticles in HDPE. Melt blending was performed at 220 °C and 30 rpm for 15 min. During the mixing period the melt temperature and torque were continuously recorded. Each nanocomposite after preparation was milled and placed in a desiccator to be prevented from moisture absorption.

2.3. Mechanical properties

Measurements of tensile mechanical properties of the prepared nanocomposites were performed on an Instron 3344 dynamometer, in accordance with ASTM D638, using a crosshead speed of 50 mm/min. Thin films of about 350 ± 25 μm were prepared using an Otto Weber, Type PW 30 hydraulic press connected with an Omron E5AX Temperature Controller, at a temperature of 220 ± 5 °C. The moulds were rapidly cooled by immersing them in water at 20 °C. From these films, dumb-bell-shaped tensile test specimens (central portions 5 × 0.5 mm thick, 22 mm gauge length) were cut in a Wallace cutting press and conditioned at 25 °C and 55–60% relative humidity for 48 h. The values of Young's modulus, yield stress, elongation at break and tensile strength at the break point were determined. At least five specimens were tested for each sample and the average values, together with the standard deviations, are reported.

Izod impact tests were performed using a Tinius Olsen apparatus in accordance with ASTM D256 method. Five measurements were conducted for each sample, and the results were averaged to obtain a mean value.

2.4. Dynamic mechanical analysis (DMA)

The dynamic thermomechanical properties of the nanocomposites were measured with a Rheometric Scientific analyzer (model Mk III). The bending method was used at a frequency of 1 Hz, a strain level of 0.04% in the temperature range of −100 to 60 °C. The heating rate was 3 °C/min. Testing was performed using rectangular bars with dimensions, approximately, 30 mm × 10 mm × 3 mm. These were prepared with a hydraulic press, at a temperature of 220 °C and a pressure of 100 bar, for a time period of 5 min. The exact dimensions of each sample were measured before the scan.

2.5. Scanning electron microscopy (SEM)

SEM was carried out using a JEOL JMS-840A scanning microscope equipped with an energy-dispersive X-ray (EDX) Oxford ISIS 300 micro-analytical system. For SEM measurements fractured surfaces as well as thin films were used. All the studied surfaces were coated with carbon black to avoid charging under the electron beam.

2.6. Differential scanning calorimetry

Thermal analysis of the nanocomposites was performed using a differential scanning calorimeter (Setaram, DSC141) calibrated with indium and zinc standards. For each measurement a sample of about 6.0 ± 0.2 mg was used, placed in a sealed aluminium pan, and heated to 180 °C at a scanning rate of 5 °C/min. From these scans the melting temperature (T_m) of the nanocomposites was measured.

2.7. Thermogravimetric analysis

Thermogravimetric analysis was carried out with a SETARAM SETSYS TG-DTA 16/18. Samples (6.0 ± 0.2 mg) were placed in alumina crucibles. An empty alumina crucible was used as reference. HDPE nanocomposites were heated from ambient temperature to 550 °C in a 50 ml/min flow of N_2 at heating rates of 5, 10 and 15 °C/min. Continuous recordings of sample temperature, sample weight, its first derivative and heat flow were performed.

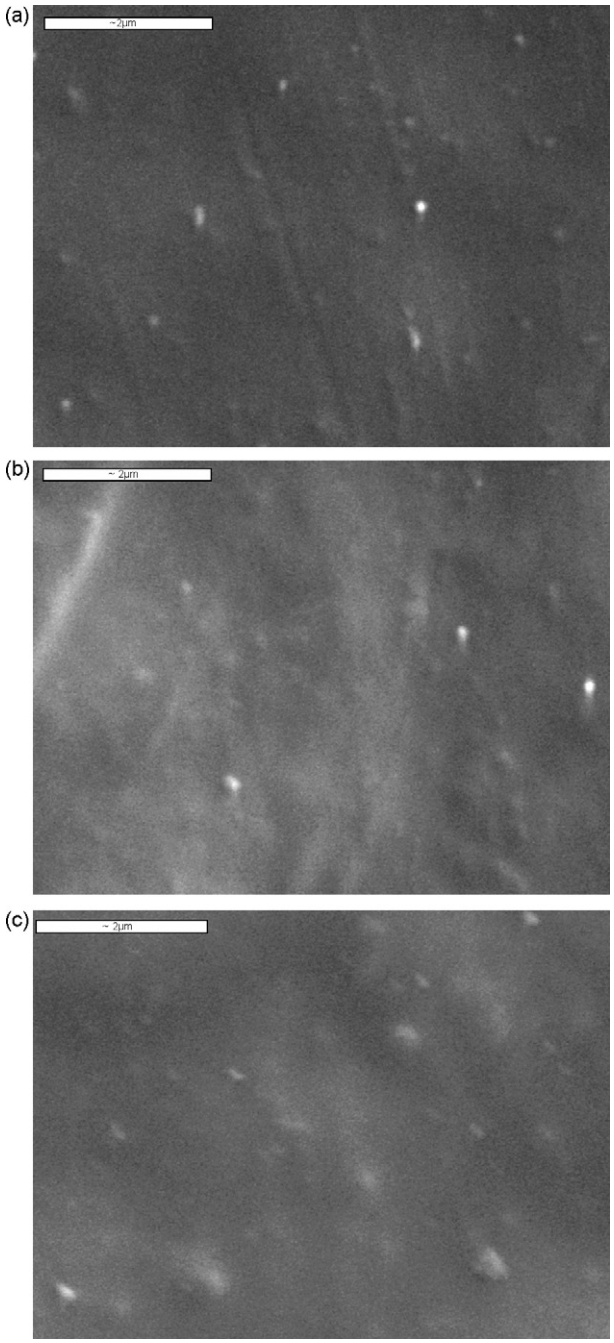

Fig. 1. SEM microphotographs of HDPE/SiO_2 nanocomposites containing (a) 1 wt.%, (b) 2.5 wt.% and (c) 5 wt.% silica nanoparticles.

3. Results and discussion

3.1. Characterization of HDPE/SiO_2 nanocomposites

The dispersion and adhesion of nanoparticles with the polymer matrix are of great importance for improving the mechanical behavior and other properties of nanocomposites. Fine control of the interface morphology of polymer nanocomposites is one of the most critical parameters to impart desired mechanical properties of such materials. In the SEM micrographs (Fig. 1), it can be seen that although SiO_2 nanoparticles were used with average particle size diameter 12 nm, these cannot be dispersed into HDPE matrix as individual nanoparticles and silica agglomerates are formed. This is in agreement with other previous studies in polyolefins like PP [29,30] and other polymers [31,32]. In all the samples these agglomerates are spherical in shape, with a diameter depending on the SiO_2 concentrations. In nanocomposites containing 1 wt.% of SiO_2 the aggregates' size is up to 150 nm, while at 2.5 and 5 wt.% of SiO_2 the sizes of aggregates are up to 200 and 350 nm, respectively. This behavior is characteristic of fumed silica and it is attributed to the strong interaction of the surface hydroxyl groups [33]. For this reason, fumed silica can be found only in aggregates, which form clusters and seems that it is very difficult to break down during melt-mixing even when high shear rates are employed as in the extruders [34].

The formation of such aggregates is also reflected to the mechanical properties of nanocomposites (Table 1). From stress–strain curves it is observed that all nanocomposites exhibit the typical cold-drawn behavior since cold drawing was appeared before the final break of the specimen. During this phenomenon tensile strength increases further and the sample is becoming milky due to the crystallization that is taking place arrived from macromolecular alignment in the direction of applied force. Tensile strength at yield point as well as at break, is slightly increased with the increase of the silica amount, which is in agreement with a previous study [35]. On the contrary, in nanocomposites containing 5 wt.% of SiO_2, a reduction was observed in both mechanical properties due to the formation of larger aggregates, as was verified from SEM micrographs. Youngs' modulus, as is expected, increases continuously by increasing SiO_2 content due to the reinforcement effect of the nanofillers in polymer matrix [36,37], while the opposite trend was recorded for impact strength values, the latter being in agreement with the already published studies in HDPE reinforced with nanoparticles [38].

The increase of stiffness of HDPE/SiO_2 nanocomposites was also recorded with DMA. Examining the storage modulus (E') of these nanocomposites it can be seen that it is higher compared to that of HDPE. It is evident from Fig. 2 that there is a remarkable increase in the modulus of neat HDPE with the incorporation of nanoparticles. This is probably due to increase in the stiffness of the matrix with the reinforcing effect imparted by the nanoparticles that allowed a greater degree of stress transfer at the interface [39].

3.2. Thermal analysis

The nanocomposites were further characterized by thermal analysis. The DSC thermograms of the melting endotherms for all studied samples show that the differences between the samples are negligible ($T_m = 126.7 \pm 0.1\,^{\circ}C$), as was also found from our previous study by using different kind of nanoparticles [2]. However, the heat of fusion is slightly reduced from 148.8 J/g in neat HDPE to 130.2 J/g in nanocomposites containing 5 wt.% SiO_2 (Table 2),

Table 1
Mechanical properties of HDPE/nanocomposites.

Material	Tensile strength at yield (MPa)	Tensile strength at break (MPa)	Youngs' modulus (MPa)	Elongation at break (%)	Impact strength (J/m)
HDPE	19.7 ± 2.3	29.9 ± 2.4	609 ± 34	770 ± 45	42 ± 5
HDPE/SiO_2 0.5 wt.%	21.5 ± 3.1	30.6 ± 2.3	650 ± 43	780 ± 23	39 ± 4
HDPE/SiO_2 1 wt.%	22.8 ± 1.9	31.9 ± 2.7	680 ± 35	760 ± 45	34 ± 5
HDPE/SiO_2 2.5 wt.%	21.7 ± 2.5	33.8 ± 1.9	725 ± 25	776 ± 52	36 ± 4
HDPE/SiO_2 5 wt.%	18.4 ± 3.3	26.8 ± 3.5	920 ± 53	540 ± 47	32 ± 3

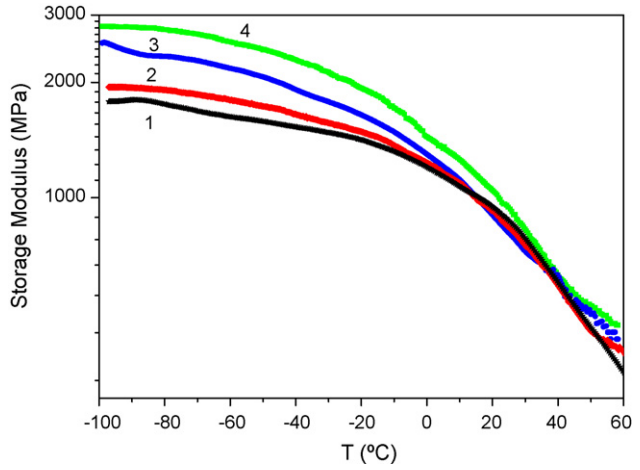

Fig. 2. Storage modulus (E') of HDPE/SiO_2 nanocomposites containing different silica content. 1: HDPE, 2: HDPE/SiO_2 1 wt.%, 3: HDPE/SiO_2 2.5 wt.% and 4: HDPE/SiO_2 5 wt.%.

which is an indication for the reduction of degree of crystallinity. This is agreement with previous studies in HDPE nanocomposites containing different nanoparticles. Sahebian et al. [40] reported that nano-sized calcium carbonate in HDPE/$CaCO_3$ nanocomposites present a significant effect on crystallinity, crystallization rates, melting point and heat of melting of HDPE. Such a behavior, was also, observed by using SiO_2 and MMT where the crystallization rates in both nanocomposites are higher, compared to neat HDPE, but the degree of crystallinity was reduced [41,42]. So, it seems that even though nanoparticles can increase the crystallization rate of polymers [43,44] they may cause a reduction on degree of crystallinity.

3.3. Thermal decomposition kinetic

Thermal degradation of HDPE/SiO_2 polymers was studied by determining their mass loss during heating. In Fig. 3 the mass loss (TG%) and the derivative mass (DTG) curves of all polymers in comparison with the curves of neat HDPE are presented, at a heating rate of 10 °C/min. From the thermogravimetric curves it is seen that all the prepared polymers present a relatively good thermostability, since no significant mass loss (<0.5%) occurred until 300 °C.

As can be followed from derivative mass curves, the maximum decomposition rates for the studied polymers were increased slightly due to the increase of SiO_2 content. Such behavior is usual in nanocomposites and has been recorded in many polymers by using different nanoparticles [16,45,46]. This stabilization is attributed to the shielding effect of nanoparticles in the evolution of formed gasses from polymer matrix, during its thermal decomposition. In order to analyze more thoroughly, the degradation mechanisms of the studied nanocomposites it is important the kinetic parameters (activation energy E and pre-exponential factor A) and the conversion function $f(\alpha)$ to be evaluated. The relationship between kinetic parameters and degree of conversion (α) can be found by using the mass loss curves in TG dynamic thermograms recorded at different heating rates such as 5, 10 and 15 °C/min. Since the differences in mass thermograms between the nanocomposites seem to be very small (Fig. 3b), the kinetic parameters were studied only for the samples with the higher content of SiO_2 (HDPE–5 wt.% SiO_2), in comparison with neat HDPE. From the recorded thermograms (Fig. 4) of HDPE/SiO_2 nanocomposite containing 5 wt.% of SiO_2 it is

Table 2
Heat of fusion of HDPE/nanocomposites.

Sample	Melting point (°C)	Heat of fusion (J/g)
HDPE	126.7	148.8
HDPE/SiO_2 0.5 wt.%	126.5	148.9
HDPE/SiO_2 1 wt.%	126.6	147.7
HDPE/SiO_2 2.5 wt.%	126.8	144.6
HDPE/SiO_2 5 wt.%,	126.7	130.2

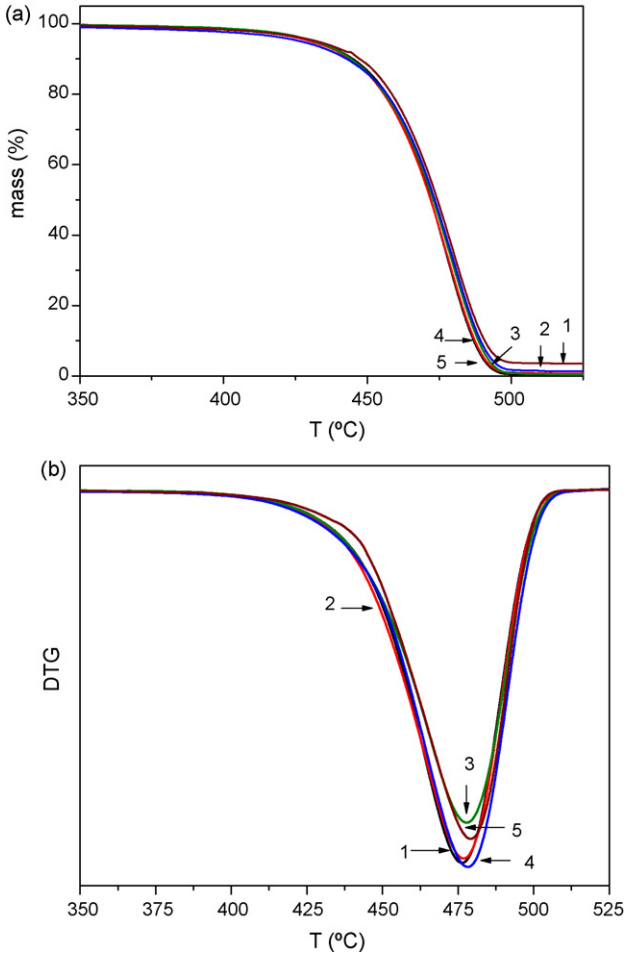

Fig. 3. TGA thermograms of HDPE/SiO_2 recorded with heating rate β = 10 °C/min, (a) mass (%) and (b) derivative mass (DTG) versus temperature. 1: HDPE, 2: HDPE/SiO_2 1 wt.%, 3: HDPE/SiO_2 2.5 wt.%, 4: HDPE/SiO_2 2.5 wt.% and 5: HDPE/SiO_2 5 wt.%.

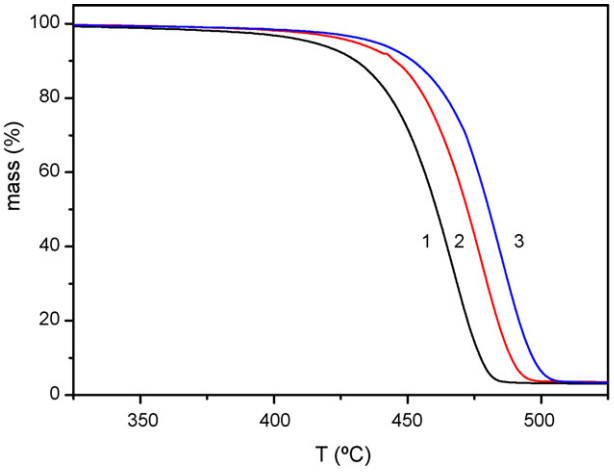

Fig. 4. HDPE–5 wt.% SiO_2. Mass (%) versus temperature for different heating rates, 1: β = 5 °C/min, 2: β = 10 °C/min and 3: β = 15 °C/min.

clear that the peak temperature where the maximum decomposition rate takes place, shifts to higher values with increasing heating rate and similar is the behavior for neat HDPE.

The activation energy, E, of thermal decomposition can be calculated by the isoconversional method of Ozawa, Flynn and Wall (OFW) [47,48] a "model free" method which assumes that the conversion function $f(\alpha)$ does not change with the alteration of the heating rate for all values of α. It involves the measuring of the temperatures corresponding to fixed values of α from experiments at different heating rates β. Therefore, plotting $\ln(\beta)$ against $1/T$ in the form of:

$$\ln(\beta) = \ln\left[\frac{Af(\alpha)}{d\alpha/dT}\right] - \frac{E}{RT}$$

should give straight lines and its slope is directly proportional to the activation energy ($-E/R$), where A is the pre-exponential factor, that is considered to be independent of temperature, E the activation energy, T the absolute temperature, and R is the gas constant. If the determined activation energy is the same for the various values of α, the existence of a single-step reaction can be concluded with certainty. On the contrary, a change of E with increasing degree of conversion is an indication of a complex reaction mechanism that invalidates the separation of variables involved in the OFW analysis [49].

For comparison reasons at Fig. 5 can be seen the dependence of the activation energy on the degree of conversion α for HDPE and HDPE/SiO_2 5 wt.%. As can be seen, all calculated values of the activation energy of HDPE/SiO_2 5 wt.% are higher than that of neat HDPE. This is evidence that SiO_2 causes stabilization in thermal decomposition of HDPE. Comparing the results from the dependence of the activation energy E on the degree of conversion α (Fig. 5) it can be seen that this dependence of E on α value can be divided into two main distinct regions. The first for values of α up to 0.3 in which E presents almost a first plateau ($0.1 < \alpha < 0.3$), and the second ($\alpha > 0.3$) in which E presents firstly a slight increase and then almost a plateau ($0.3 < \alpha < 1$). This dependence of E on α for a sample is an indication of a complex reaction with the participation of at least two different mechanisms. Although the "two mechanisms" – as a result of the increasing E with α – is a rather typical phenomenon for many polymers [50,51] this conclusion is based on the multistep TG curve. However, this is not clear in our studied samples and the conclusion is extracted mainly through the dependence of E versus α.

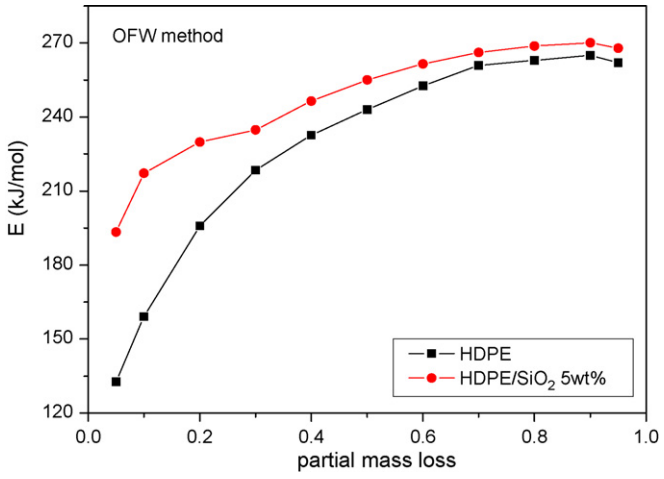

Fig. 5. The dependence of the activation energy on the degree of conversion (partial mass loss) for the HDPE/SiO_2 5 wt.% resulted from OFW method. The lines are guide to the eye.

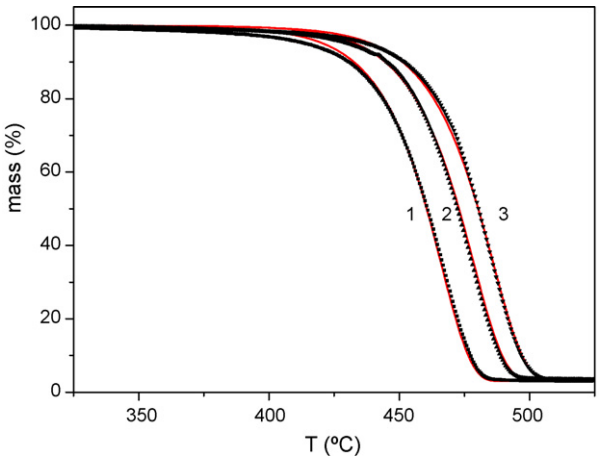

Fig. 6. Fitting and experimental data TG curves of HDPE/SiO_2 5 wt.% for one reaction mechanism and different heating rates. 1: $\beta = 5$ °C/min, 2: $\beta = 10$ °C/min and 3: $\beta = 15$ °C/min.

In order to determine the nature of the mechanism or mechanisms through the comparison of the experimental and theoretical data, initially it is considered that the degradation of the studied samples can be described only by a single mechanism, without presuming the exact mechanism. If the results of the identification with the help of this single mechanism could not be considered as satisfactory then, knowing this mechanism ($f(\alpha)$), the kinetic parameters and the conversion function of the other mechanism can be determined, in order to obtain a better agreement between experimental and theoretical data. To determine the conversion function $f(\alpha)$ we used a method referred to as the "model fitting method" [52–54]. This method, that does not assume the knowledge of E and $f(\alpha)$ in advance, was applied simultaneously on the experimental data taken at the heating rates $\beta = 5$, 10 and 15 °C/min. It has been shown that the "model fitting method" applied to multiple heating rate data gives activation energies similar to the values estimated by the isoconversional methods [55]. For the fitting 16 different kinetic models were used. In Fig. 6 the results of this fitting for HDPE/SiO_2 5 wt.% can be seen. The form of the conversion function, obtained by fitting, is the mechanism of autocatalysis n-order $f(\alpha) = (1-\alpha)^n(1 + K_{cat}X)$ where K_{cat} is a constant and X the reactants. The parameters of the mechanism were: the pre-exponential factor $\log A\ (s^{-1}) = 15.2$, the activation energy $E = 249.9$ kJ/mol, the exponent value n is equal to 0.8, and the correlation coefficient was 0.9997. The value of the activation energy is between the limits of the calculated values from the OFW method. As it can be seen, the fitting to the experimental data is good for a very large range of the mass loss and only at the first region of mass loss (<20%) small variations can be recognized.

In our previous article [2] in which the kinetics of the thermal degradation of neat HDPE has been studied, the quality of the fitting with one mechanism was worst from the analogous one of the HDPE/SiO_2 5 wt.%. The parameters for the same mechanism for HDPE were: the pre-exponential factor $\log A\ (s^{-1}) = 14.3$, the activation energy $E = 239.1$ kJ/mol, the exponent value n is equal to 0.74, and the correlation coefficient was 0.999. Due to the quality of the fitting for the kinetic description of the HDPE two mechanisms were used. So, two mechanisms also used for HDPE/SiO_2 5 wt.% sample. For the determination of the two different mechanisms the following are assumed: (a) the two mechanisms follow each other and (b) the unknown mechanism corresponds to the first stage of mass loss. An improvement of fitting is observed and the agreement of experimental and theoretical results (Fig. 7) is remarkable, verifying that the polymer is degraded by two different mechanisms during its thermal decomposition. The kinetic model of the first decompo-

Table 3
Calculated values of activation energy, pre-exponential factor and exponent n for HDPE and HDPE/SiO_2 5 wt.%.

Sample	Activation energy (kJ/mol)	Pre-exponential factor ($\log A$)	Reaction order (n)	$\log K_{cat}$
First reaction mechanism—reaction model Cn				
HDPE	140.0	7.9	0.27	−4.7[a]
HDPE/SiO_2 5 wt.%	201	12.59	0.9	−5.1[a]
Second reaction mechanism—reaction model Cn				
HDPE	260.0	15.8	1.01	0.47
HDPE/SiO_2 5 wt.%	266	16.36	0.96	0.13

[a] Large negative values.

Table 4
Calculated values of activation energy, pre-exponential factor and exponent n for HDPE and HDPE/SiO_2 5 wt.%.

Sample	Activation energy (kJ/mol)	Pre-exponential factor ($\log A$)	Reaction order (n)	$\log K_{cat}$
First reaction mechanism—reaction model Fn				
HDPE	140	7.90	0.27	
HDPE/SiO_2 5 wt.%	201	12.55	0.83	
Second reaction mechanism—reaction model Cn				
HDPE	260	15.80	1.01	0.47
HDPE/SiO_2 5 wt.%	266	16.35	0.97	0.17

sition mechanism is also autocatalysis nth-order (reaction model Cn). The data of the fitting for the studied nanocomposites are presented in Table 3. In this stage of identification for the best possible results, we left the parameters (E, A, and n) of both the examined mechanisms to be recalculated and the correlation coefficient was 0.9998. The results of the dependence of the activation energy on the degree of conversion, α, are in well agreement with mass loss. The first degradation mechanism is attributed to small mass loss, while the second degradation mechanism is attributed to the main mass loss and is, also, autocatalysis nth-order.

As it can be seen in Table 3 the value of $\log(K_{cat})$ is a very large negative number, so the term K_{cat} is a very small number, almost zero. For this reason the reaction model is analogous to the nth-order model (reaction model Fn). The results of the fitting with the mechanisms Fn–Cn are presented in Table 4. The quality of the fitting is as good as with the combination of the mechanisms Cn–Cn. The differences of the calculated values are negligible. Thus, it can be concluded that the first decomposition mechanism can be adequately described as by nth-order mechanism (Fn) while the second one as autocatalysis nth-order (Cn). The activation energies are completely different, since the first mechanism has lower activation energy. Comparing the activation energies of HDPE and HDPE/SiO_2 nanocomposites it can be seen, that SiO_2 nanoparticles have a more pronounced effect on the first mechanism, which is corresponding to the first stages of HDPE decomposition. As can be seen the activation energy of HDPE first reaction mechanism is 140 kJ/mol while after the addition of SiO_2 nanoparticles this is increased to 201 kJ/mol. In the second degradation mechanism, which corresponds to the main mass loss, the effect of silica nanoparticles is lower since the activation energy was enhanced only by 6 kJ/mol. So, it seems that when the decomposition of the polymer is extensive the addition of nanoparticles cannot depress the decomposition rate.

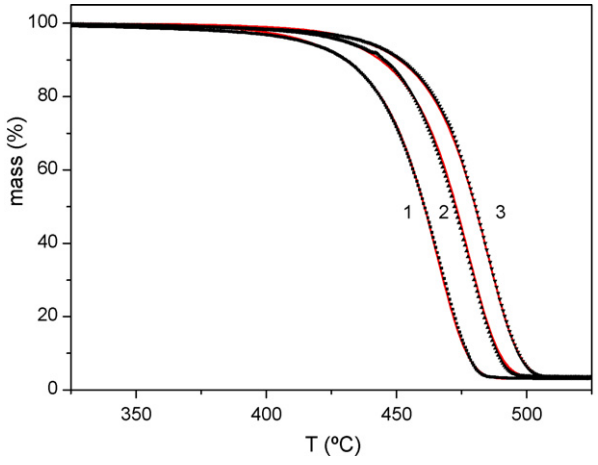

Fig. 7. Fitting and experimental data TG curves of HDPE/SiO_2 5 wt.% for two reaction mechanisms and different heating rates. 1: $\beta = 5\,^{\circ}C/min$, 2: $\beta = 10\,^{\circ}C/min$ and 3: $\beta = 15\,^{\circ}C/min$.

4. Conclusions

The studied HDPE/SiO_2 nanocomposites exhibited enhanced mechanical properties such as tensile strength at break and Youngs' modulus while increasing the amount of SiO_2 nanoparticles reduced impact strength. Thermal degradation of HDPE can be described with two different mechanisms. The first degradation mechanism is attributed to small mass loss and is nth-reaction order. The second degradation mechanism is attributed to the main mass loss and is autocatalysis nth-order. The activation energy of the first mechanism is 140 kJ/mol and for the second is 260 kJ/mol for neat HDPE. The addition of SiO_2 nanoparticles enhances the thermal stability of HDPE. Thermal decomposition of HDPE nanocomposites takes place also with two mechanisms, as neat HDPE. However, both mechanisms have higher activations energies (201 and 266 kJ/mol for HDPE/SiO_2 5 wt.%), which is a further evidence of thermal stabilization effect of SiO_2 nanoparticles. Comparing the activation energies of both mechanisms it can be seen that the effect of SiO_2 nanoparticles is more pronounced in the first mechanism than in the second.

References

[1] P. Galli, G. Vecellio, J. Appl. Polym. Sci. Part A: Polym. Chem. 42 (2004) 396.
[2] K. Chrissafis, K.M. Paraskevopoulos, D. Bikiaris, submitted for publication.
[3] Y.C. Ou, F. Yang, Z.Z. Yu, Polym. J. Sci. Part B: Polym. Phys. 36 (1998) 789.
[4] K.H. Wang, C.M. Koo, I.J. Chung, J. Appl. Polym. Sci. 89 (2003) 2131.
[5] Y.H. Lee, B. Park, M. Sain, M. Kontopoulou, W. Zheng, J. Appl. Polym. Sci. 105 (2007) 1993.
[6] D. Chu, Q. Nguyen, D.G. Baird, Polym. Compos. 28 (2007) 499.
[7] K.H. Wang, M. Xu, Y.S. Choi, I.J. Chung, Polym. Bull. 46 (2001) 499.
[8] K.D. Min, M.Y. Kim, K.Y. Choi, J.H. Lee, S.G. Lee, Polym. Bull. 57 (2006) 101.
[9] S. Filippi, C. Marazzato, P. Magagnini, A. Famulari, P. Arosio, S.V. Meille, Eur. Polym. J. 44 (2008) 987.
[10] J.H. Lee, S.K. Kim, N.H. Kim, Scripta Mater. 55 (2006) 1119.

[11] M. Trujillo, M.L. Arnal, A.J. Müller, E. Laredo, S. Bredeau, D. Bonduel, Ph. Dubois, Macromolecules 40 (2007) 6268.
[12] F. Wu, X. He, Y. Zeng, H.M. Cheng, Appl. Phys. A 85 (2006) 25.
[13] Y. Zou, Y. Feng, L. Wang, X. Liu, Carbon 42 (2004) 271.
[14] Y. Zhong, D. Janes, Y. Zheng, M. Hetzer, D.D. Kee, Polym. Eng. Sci. 7 (2007) 1101.
[15] M.A. Osman, J.E.P. Rupp, U.W. Suter, J. Mater. Chem. 15 (2005) 1298.
[16] K. Chrissafis, G. Antoniadis, K.M. Paraskevopoulos, A. Vassiliou, D.N. Bikiaris, Comp. Sci. Technol. 67 (2007) 2165.
[17] K. Chrissafis, K.M. Paraskevopoulos, G.Z. Papageorgiou, D.N. Bikiaris, J. Appl. Polym. Sci. 110 (2008) 1739.
[18] C.H. Wu, C.Y. Chang, J.L. Hor, S.M. Shih, L.W. Chen, F.W. Chang, Waste Manage. 13 (1993) 221.
[19] R. Knumann, H. Bockhorn, Combust. Sci. Technol. 101 (1994) 285.
[20] H. Bockhorn, A. Hornung, U. Hornung, D. Schawaller, J. Anal. Appl. Pyrol. 48 (1999) 93.
[21] H. Bockhorn, A. Hornung, U. Hornung, J. Anal. Appl. Pyrol. 50 (1999) 77.
[22] J.W. Park, S.C. Oh, H.P. Lee, H.T. Kim, K.O. Yoo, Polym. Degrad. Stabil. 67 (2000) 435.
[23] L. Ballice, Fuel 80 (2001) 1923.
[24] J. Yang, R. Miranda, C. Roy, Polym. Degrad. Stabil. 73 (2001) 455.
[25] A.S. Araujo, V.J. Fernandes Jr., G.J.T. Fernandes, Thermochim. Acta 392–393 (2002) 55.
[26] Z. Gao, I. Amasaki, M. Nakada, J. Anal. Appl. Pyrol. 67 (2003) 1.
[27] S. Kim, E.S. Jang, D.H. Shin, K.H. Lee, Polym. Degrad. Stabil. 85 (2004) 799.
[28] F.S.M. Sinfronio, J.C.O. Santos, L.G. Pereira, A.G. Souza, M.M. Conceicao, V.J. Fernandes Jr., V.M. Fonseca, J. Therm. Anal. Calorim. 79 (2005) 393.
[29] D. Bikiaris, A. Vassiliou, E. Pavlidou, G.P. Karayannidis, Eur. Polym. J. 41 (2005) 1965.
[30] D.N. Bikiaris, G.Z. Papageorgiou, E. Pavlidou, N. Vouroutzis, P. Palatzoglou, G.P. Karayannidis, J. Appl. Polym. Sci. 100 (2006) 2684.
[31] K. Chrissafis, K.M. Paraskevopoulos, G.Z. Papageorgiou, D. Bikiaris, J. Appl. Polym. Sci. 110 (2008) 1739.
[32] D. Bikiaris, V. Karavelidis, G.P. Karayannidis, Makromol. Rapid Commun. 27 (2006) 1199.
[33] S. Sinha Ray, M. Okamoto, Prog. Polym. Sci. 28 (2003) 1539.
[34] A. Vassiliou, D. Bikiaris, E. Pavlidou, Macromol. React. Eng. 1 (2007) 488.
[35] M.Q. Zhang, M.Z. Rong, H.B. Zhang, K. Friedrich, Polym. Eng. Sci. 43 (2003) 490.
[36] S. Kanagaraj, F.R. Varanda, T.V. Zhil'tsova, M.S.A. Oliveira, J.A.O. Simões, Comp. Sci. Technol. 67 (2007) 3071.
[37] W. Tang, M.H. Santare, S.G. Advani, Carbon 41 (2003) 2779.
[38] M. Tanniru, Q. Yuan, R.D.K. Misra, Polymer 47 (2006) 2133.
[39] V. Vladimirov, C. Betchev, A. Vassiliou, G. Papageorgiou, D. Bikiaris, Comp. Sci. Technol. 66 (2006) 2935.
[40] S. Sahebian, S.M. Zebarjad, S.A. Sajjadi, Z. Sherafat, A. Lazzeri, J. Appl. Polym. Sci. 104 (2007) 3688.
[41] T.G. Gopakumar, J.A. Lee, M. Kontopoulou, J.S. Parent, Polymer 43 (2002) 5483.
[42] Q. Jiasheng, J. Mater. Sci. 38 (2003) 2299.
[43] A. Vassiliou, G.Z. Papageorgiou, D.S. Achilias, D.N. Bikiaris, Macromol. Chem. Phys. 21 (2007) 364.
[44] G.Z. Papageorgiou, D.S. Achilias, D.N. Bikiaris, G.P. Karayannidis, Thermochim. Acta 427 (2005) 117.
[45] K. Chrissafis, K.M. Paraskevopoulos, S.Y. Stavrev, A. Docoslis, A. Vassiliou, D.N. Bikiaris, Thermochim. Acta 465 (2007) 6.
[46] A. Vassiliou, D. Bikiaris, K. Chrissafis, K.M. Paraskevopoulos, S.Y. Stavrev, A. Docoslis, Comp. Sci. Technol. 68 (2008) 933.
[47] T. Ozawa, Bull. Chem. Soc. Jpn. 38 (1965) 188.
[48] J. Flynn, L.A. Wall, J. Polym. Sci. Part B: Polym. Lett. 4 (1966) 232.
[49] T. Ozawa, J. Therm. Anal. 2 (1970) 30.
[50] J.D. Peterson, S. Vyazovkin, C.A. Wight, Macromol. Chem. Phys. 202 (2001) 775.
[51] S. Vyazovkin, Anal. Chem. 80 (2008) 4301.
[52] S. Vyazovkin, C.A. Wight, Thermochim. Acta 340 (1999) 53.
[53] S. Vyazovkin, N. Sbirrazzuoli, Macromol. Rapid Commun. 27 (2006) 1515.
[54] K. Chrissafis, J. Therm. Anal. Calorim 95 (2009) 273.
[55] A. Burnham, Thermochim. Acta 355 (2000) 165.